

A Finite Element Approach to the Design of Flexible Pavements in Canada

Reza Kakavand¹, Mohammad Shafiee², Omran Maadani³, Amin Komeili^{4*}

¹PhD Student, University of Guelph, ON, Canada, email: rkakavand@uoguelph.ca

²Research Officer, National Research Council Canada, email: Mohammad.Shafiee@nrc-cnrc.gc.ca

³Research Officer, National Research Council Canada, email: Omran.Maadani@nrc-cnrc.gc.ca

⁴Assitant Professor, University of Guelph, ON, Canada, email: akomeili@uoguelph.ca

Abstract

The design of cost-effective, long-lasting flexible pavements is of high importance in Canada, where daily and seasonal temperature varies significantly. Moreover, the abrupt changes in the global climate and its inverse impacts on transport infrastructures over the last decade require planning for necessary adaptations to mitigate those effects. More research should be conducted to address the potential impacts of climate change on the flexible pavement design. A mechanistic analysis that considers thermomechanical loads could be a tool to study the possibility of variations in frequency or severity of pavement failure due to climate change. Such a model, when is fed with site-specific material properties, traffic load, temperature profile, and pavement parameters, would more accurately predict the performance, serviceability and safety requirements. The pavement design may involve identifying tens of parameters, which makes it complex for pavement engineers. The current study presents a finite element analysis of flexible pavements to evaluate thermal- and traffic-induced stresses for two selected highway cross-sections in Ontario and British Columbia. The behavior of the asphalt concrete layer was considered a linear viscoelastic. The unbound materials layers of the flexible pavement were considered elastic. The change in layers stiffness due to air temperature was simulated by considering temperature-dependent material properties. Two failure criteria, fatigue cracking and permanent deformation, were considered for computing the allowable number of load repetitions. The results showed that site-specific temperatures (historical or projected or both) could have a profound effect on this allowable number, and therefore, on the design life of the pavement.

Keywords: Finite Element Analysis; Flexible Pavement; temperature effect; Canada.

1. Introduction

Transportation infrastructure systems are designed for local climate using the historical data and maybe making projections based on its history within the locality. Should any profound future climate change occur, transportation will be affected through changes in weather extremes that are reflected in temperature, precipitation level, freeze-thaw cycles, wind speed, and rising sea levels. Canada's Changing Climate Report (CCCR) 2019 indicated that Canada's annual temperature change has risen at a rate of 1.7 °C, roughly double the global mean rate [1]. More importantly, Canada would see an annual temperature change of 6°C under a high emission rate scenario (RCP 2.6) that is mainly attributed to human activities in the form of greenhouse gas emission [2]. Climate change now is more than a potential threat for Canada; rather, it is a ubiquitous man-made problem with destructive effects on natural resources, ecosystems, quality of life, and many more to mention, including the transportation infrastructure systems. Therefore, the design of pavement systems should change from static to an evolving process that accounts for climate change and physical properties of road materials. It is widely recognized that transitory temperature can cause pavement distress in hot mix asphalt (HMA). The temperature gradient from the top and bottom of the HMA can induce volumetric strains, which lead to the development of tensile stresses in conjunction with traffic loading. This could sway the rheology of asphalt binder. Apart from the abovementioned transitory changes, extreme events of very cold or and warm temperatures outside the design assumptions would expedite fatigue failure [3]. Hence, both projected and historical temperature changes are crucial in calculating the fatigue damage accumulation of HAM. The current design method does not accurately account for both the historical and projected temperature of the flexible resulted in failures of the pavement structure. There is also room for material improvement by introducing nanoclay, nanocarbon, and nanosilica, as a way to improve the rheological properties of asphalt and its mechanical properties such as tensile strains and dynamic modulus [4, 5]. The Mechanistic-Empirical Pavement Design Guide (M-EPDG) incorporates the mechanistic approach to the experimental

approach, which was integrated into the AASHTOWare Pavement ME Design software for simulating pavement performance. The Enhanced Integrated Climate Model (EICM) was incorporated in M-EPDG's to simulate changes in the behaviour and characteristics of pavement and subgrade materials with considering the impact of climate change over the design period [6]. However, it uses the historical climatic data that do not accurately represent the projected climatic condition anymore. Moreover, to use it with confidence that required intensive work of calibration, that makes us carry on this study. In light of climate change and its new reality, this study aimed to conduct a sensitivity analysis on the effect of temperature change on the fatigue cracking (N_f), and permanent deflection (N_d) of HMA using a 2D nonlinear material formulation implemented in MATLAB.

2. Method

In this study, a 2D layer-wise finite element (FE) was developed to represent the HMA layers. The equilibrium equations were coupled with a two-dimensional heat transfer equation to account for the temperature gradient. Although the program was structured such that it can be extended to 3D, we used a 2D model for this study to decrease the computational cost, because the resources required to perform a nonlinear 3D analysis are usually warranted only for special situations such as unusual geometries. To tailor distresses to meet local pavement conditions, a sensitivity analysis was conducted to locally calibrate N_f and N_d parameters. Results obtained from the changing temperature were compared. The methodology is illustrated in the flowchart in Figure 1. Two different pavements, one from Ontario (ON) and the other from British Columbia (BC), were selected. The pavement selected from ON was 1806 SHRP_ID with the state code of 87 (address: ON-404, Gormley, ON L0H 1G0, Canada) with Average Annual Daily Traffic (AADT) of 22890. The second from BC was referred to as 6006 SHRP_ID with the 82 state code (address: Vancouver-Blaine Hwy, Delta, BC V4K 3N3, Canada) with AADT of 16620. The selected pavement cross-sections consisted of four layers (including subgrade). The asphalt layer was assumed viscoelastic, while other layers were assumed to be linearly elastic. Historical data were used in a multi-layer pavement model developed in the present study to compute the allowable number of load repetitions.

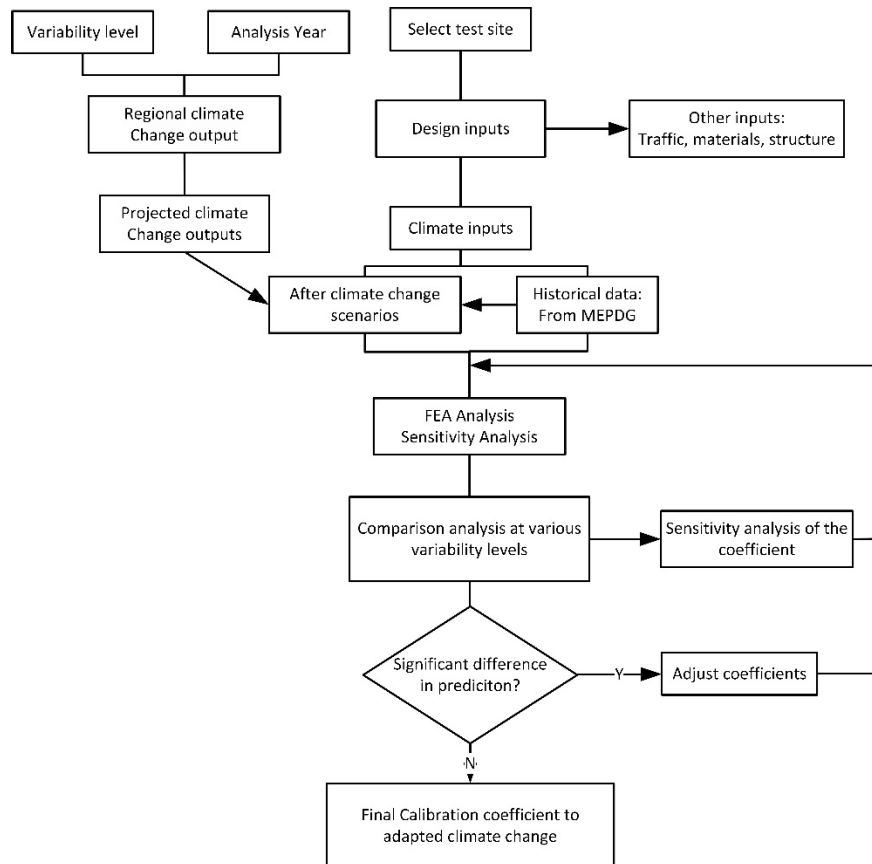


Figure 1. The flowchart illustration of the methodology in sensitivity analysis to locally calibrated distresses.

2.1. Geometry

Thicknesses of the asphalt (original surface layer), base, and subbase were taken from INFOPAVE website [7], and the thickness of the subgrade was set to be 3.6 times more than the sum of thicknesses of the other layers (Table 1).

Table 1. The thickness of HMA layers in the FE model

	Thickness (mm)	
	The Ontario pavement	The British Columbia pavement
HMA layer	167	145
Base	180	208
Subbase	965	604
Subgrade	4723	3445

2.2. Material

The viscoelastic properties of the pavement were selected from the INFOPAVE website [7]. On this website, the dynamic moduli of pavements as a function of frequency are reported. We converted the dynamic moduli to relaxation modulus $E(t)$ using the following equation [8]:

$$|E^*| = \sqrt{\left(E_e + \sum_{i=1}^m \frac{\omega^2 \rho_i^2 E_i}{\omega^2 \rho_i^2 + 1}\right)^2 + \left(\sum_{i=1}^m \frac{\omega \rho_i E_i}{\omega^2 \rho_i^2 + 1}\right)^2} \quad (1)$$

$$E(t) = E_e + \sum_{i=1}^m E_i \cdot e^{(-t/a_T \rho_i)} \quad (2)$$

where E^* is the dynamic modulus; ω is frequency; and ρ and E are relaxation modulus coefficients. Subscript e denotes the value of the relaxation modulus at infinite time, and i is the number of coefficients considered for the Prony series to define the relaxation modulus. Figure 2 illustrates fitted curves on the dynamic modulus. a_T is a shift function that accounts for the effect of temperature that is given by [9]:

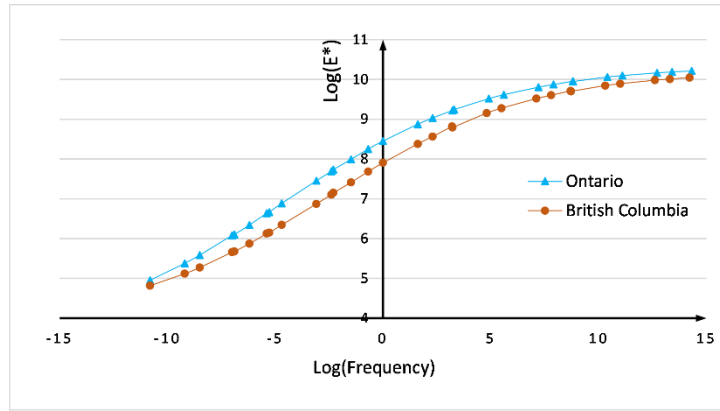


Figure 2. Curve fitting on the dynamic modulus points of the two selected cross-section pavements.

$$\text{Log}(a_T) = aT^2 + bT + c \quad (3)$$

where a , b and c are shift function coefficients, and T is the temperature in Celcius. These coefficients are given in Table 2. As temperature decreases from 40 to -20 °C, the relaxation modulus $E(t)$ increases.

Table 2. The shift function coefficients that were used in equation (3).

	Shift function coefficients		
	a	b	c
Ontario	0.001575	-0.3744	7.21
British Columbia	0.001543	-0.3712	7.131

The final results for the relaxation modulus parameters ρ_i and E_i in equation (2) were listed in Table 3. The Poisson's ratio for the asphalt was assumed 0.35 [10]. The Elastic moduli and Poisson's ratio of the other layers are given in Table 4 [10].

Table 3. Relaxation modulus (MPa) and thermal expansion ($^{\circ}\text{C}^{-1}$) (11) coefficients.

i	The Ontario pavement		The British Columbia pavement	
	E_i	ρ_i	E_i	ρ_i

1	2948	3.37E-06	2910	3.61E-06
2	3674	4.77E-05	3000	4.62E-05
3	4250	0.0004936	3000	2.65E-04
4	3656	0.004144	4290	1.78E-03
5	3193	0.0266	3000	1.03E-02
6	2288	0.161	3880	5.10E-02
7	1480	1.197	3320	4.08E-01
8	754.3	9.053	2050	3.76E+00
9	361	75.87	1030	3.76E+01
10	168.3	683.1	404	4.64E+02
11	83.74	8013	160	6.11E+03
		$E_e=147$	$E_e=124$	
		$\alpha= 2.5e-5$	$\alpha= 2.5e-5$	

Table 4. Material properties of the base, subbase, and subgrade

	Elastic moduli (MPa)	Poisson's ratio
Base	276	0.35
Subbase	100	0.35
Subgrade	50	0.25

2.3. Finite Element Analysis

The pavement was modeled as a 14000 mm width rectangle and was meshed using 897 4-noded rectangular elements. These elements are 2-D and, in the current research, represent a cross-section of the pavement perpendicular to its length. The plane strain condition was assumed considering the fact that the third dimension of the pavement (its length) is so long [11]. An 80-kN single standard axle (*Figure 3*) was applied on the pavements for 0.1 seconds. Because of the symmetry of the problem, only half of the cross-section was simulated (*Figure 4*). The pavement sideline was fixed horizontally to satisfy the symmetry condition, and the bottom side was fixed.

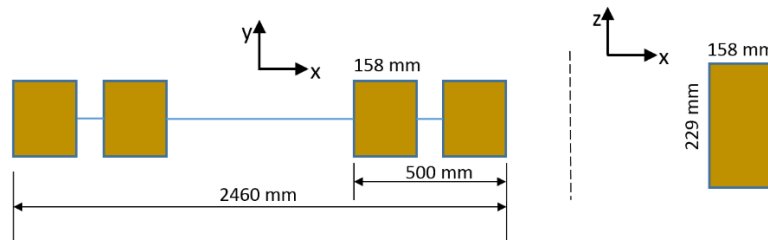


Figure 3. An 80-kN single axle load was used for the simulation [12]. Note that this axle has four wheels. The rectangle on the right side illustrates the contact area of one wheel.

2.4. Effect of climate change

To quantify the impact of temperature change, a sensitivity analysis was conducted by varying the temperature at an interval of 5 degrees from -20 to +40 °C; a total of 13 scenarios were considered for each selected cross-section. The thermal stress of the asphalt layer was calculated based on the temperature difference between the simulated temperature and a reference temperature at 21.1 °C. The base, subbase, and subgrade were assumed to be at the reference temperature.

2.5. Pavement performance

The allowable number of 80-kN repetitions was calculated at different temperatures of the asphalt using the fatigue cracking N_f and permanent deformation N_d criteria [12] that are given:

$$N_f = 0.0796(\varepsilon_t)^{-3.291}(E)^{-0.854} \quad (4)$$

$$N_d = 1.365 \times 10^{-9}(\varepsilon_c)^{-4.477} \quad (5)$$

where N_f and N_d are the allowable number of load repetitions, ε_t is the maximum tensile strain (in the present study $\varepsilon_x = \varepsilon_t$) at the bottom of the asphalt layer, ε_c is the maximum compressive strain (in the present study $\varepsilon_y = \varepsilon_c$) on the top of the subgrade, and E is the relaxation modulus of the asphalt (in psi) at the respected time.

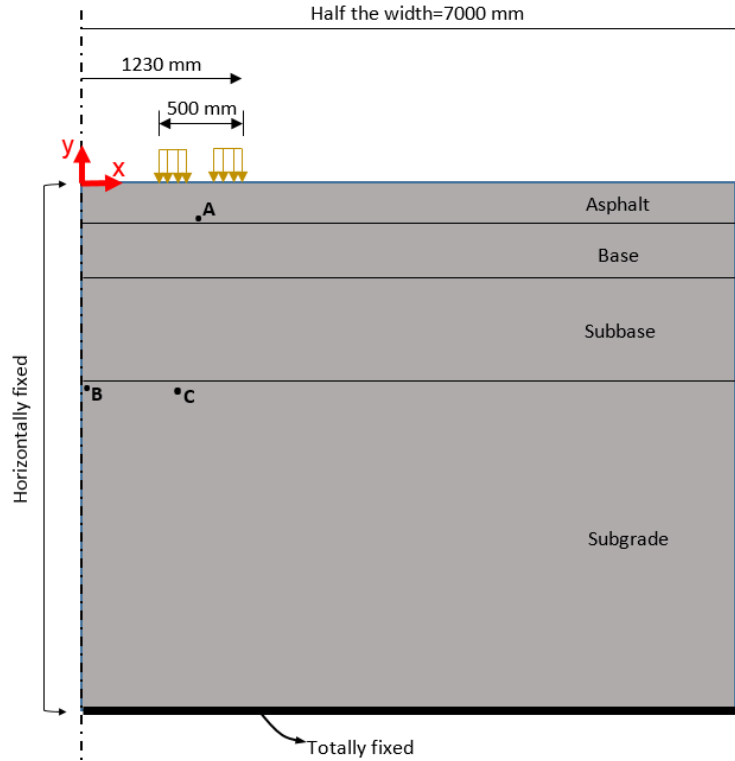


Figure 4. The configuration of the pavement model in the finite element analysis. Two surface forces (tractions) on the top represent two wheels of the axle.

3. Results

After the 0.1-second simulation, the maximum tensile strain at the bottom of the asphalt layer occurred between the two wheels (point A in Figure 4). Figure 5 shows the absolute value of deflection, tensile strain ε_x , and stress components at the bottom of the asphalt at point A. The mechanical response of the asphalt was affected by the temperature change. At the bottom of the asphalt, the least deflection is seen to be at around 15 or 21 °C, followed by an increase when temperature either increases or decreases. The tensile strain ε_x follows the same trend (Figure 5-b). However, the stresses decreased with temperature increase (Figure 5-c and -d). The ON pavement model deflected more than the BC pavement model in each of the asphalt and subgrade layers. At colder temperatures, the deflection of the asphalt layer of ON pavement was more sensitive to temperature change than the BC counterpart. An opposite relation was shown at higher temperatures.

Figure 6 shows the maximum deflection (point B in Figure 4) and the maximum compressive strain ε_y (point C in Figure 4) on the top of the subgrade layer. The results imply that the change in the temperature of asphalt would induce a different mechanical response in the subgrade. The compressive strains ε_y at point C increases as the temperature increases (Figure 6-b). The contour plots of ε_y were plotted in Figure 7 at two extreme temperatures to better investigate this behavior. At higher temperatures (Figure 7-b and 7-d), the compressive strain distributions are localized under the tire's footprint that resulted in a high strain at point C. In contrast, at lower temperatures (Figure 7-a and 7-c), a distribution of deformations in the subgrade is observed.

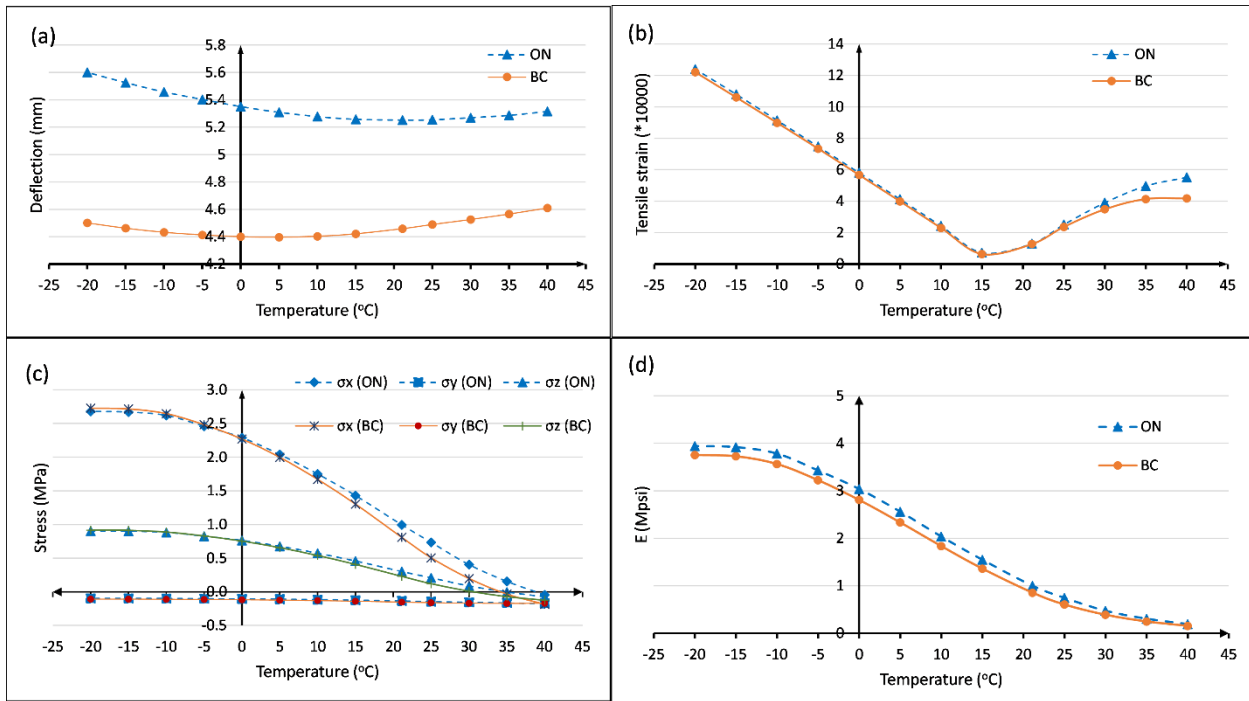


Figure 5. (a) The maximum deflection, (b) tensile strain (ϵ_x), (c) compressive stress, and (d) relaxation modulus at the bottom of the asphalt layer (point A in Figure 4) after 0.1s of loading.

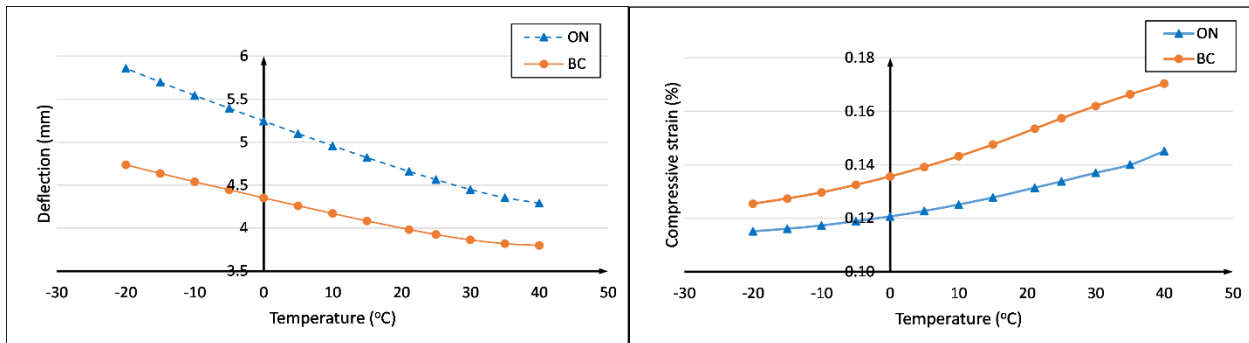


Figure 6. (a) The maximum deflection (point B in Figure 4) and (b) the compressive strain (ϵ_y) (point C in Figure 4) on the top of subgrade. The temperature change applied only to the asphalt layer. Layers below the asphalt layer were assumed to be at the room temperature of 21 °C.

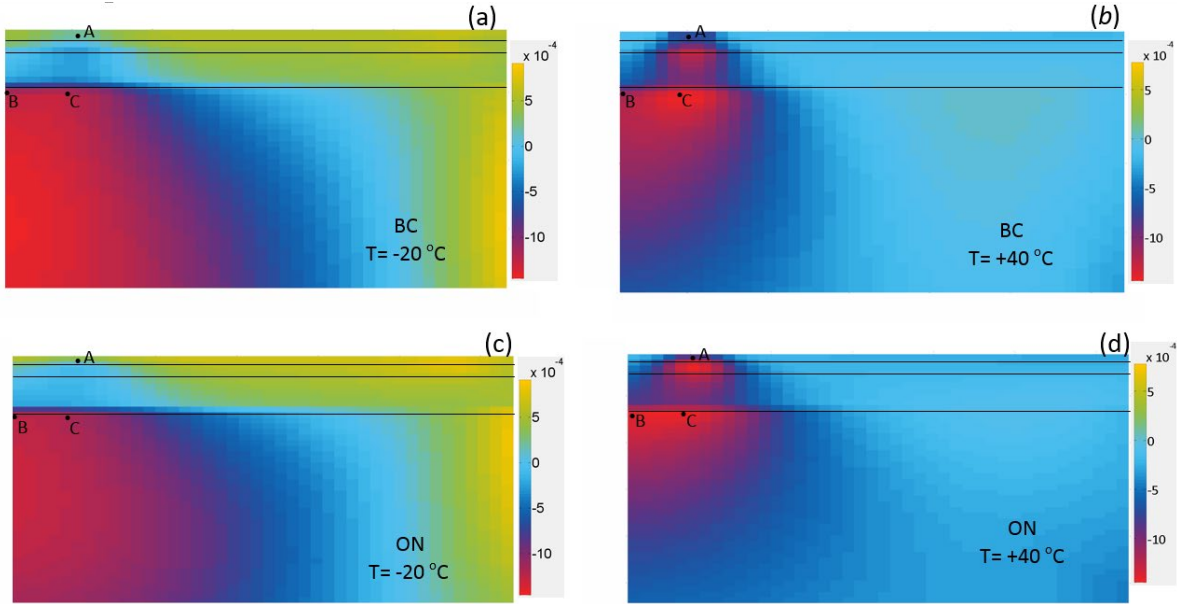


Figure 7. The contour plots of compressive strain (ϵ_y) after a 0.1-second simulation at two extreme temperatures. At point C, ϵ_y is smaller at $T=-20^\circ\text{C}$ compare to $T=+40^\circ\text{C}$ because at extreme temperatures, the asphalt layer is more rigid, and the transferred load to the subgrade is distributed.

Figure 8 illustrates the allowable number of 80-kN repetitions versus the temperature. The figure clearly shows that at higher temperatures, the allowable number is much higher when the failure N_F criterion is based on fatigue cracking. However, this distinction pales as the temperature decreases, and at -10°C , the allowable number based on permanent deformation N_d surpasses the allowable number based on fatigue cracking. At lower temperatures, these results are very similar in the ON and BC, while at high temperatures, a larger allowable number of repeated loads was obtained for the BC pavement model. Yet, generally, both states show identical trends.

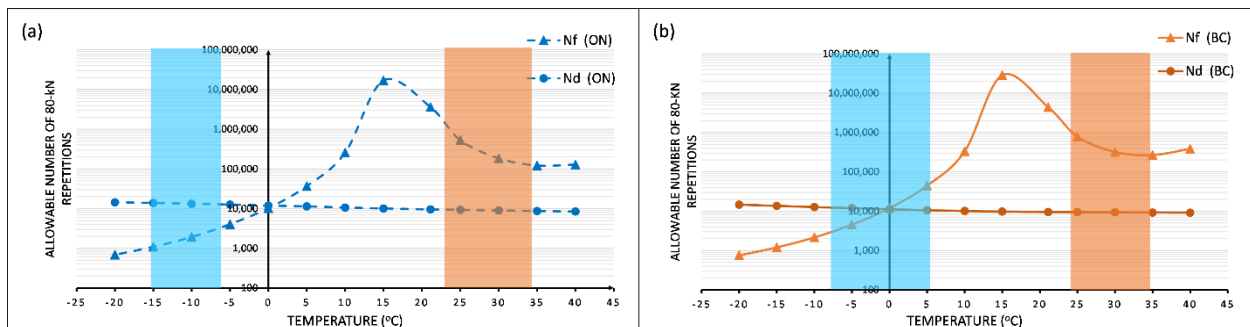


Figure 8. The allowable number of 80-kN repetitions as a function of temperature ($^\circ\text{C}$) for (a) ON pavement model and (b) BC pavement model. Three different failure criteria are plotted: the allowable number of 80-kN repetitions to limit fatigue cracking (N_f), and permanent deformation (N_d). The blue and orange shades show the range of seasonal temperatures in the winter and summers, respectively.

4. Discussion

In this research, the effect of temperature on the allowable number of 80-kN repetitions was investigated using a finite element pavement model. One pavement from ON and the other one from BC were chosen, each of which had four layers, including subgrade. The asphalt layer was considered viscoelastic, while

the other layers were linearly elastic. 4-noded rectangular elements were used to model the pavements with a plane strain approach. From the third dimension, this element assumes that the pavement is very long (which conforms to reality), but the wheels of an axle are not as long as the pavement length. This issue can be tackled if 3-D elements, such as hexagonal elements, are used. However, 2-D elements can reduce the computational time significantly that they have aroused interest among researchers and software developers. Therefore, the next step for such research can be to estimate an equivalent axle in a plane strain problem for the 80-kN axle in a 3-D problem.

The deflection at the bottom of asphalt was minimum for temperatures in the range of 15 or 21 °C (*Figure 5-a*). As temperature changes, two parameters vary with opposite effects on the deflection of the asphalt layer: thermal expansion and relaxation modulus. Increasing the temperature will expand the asphalt and will reduce its relaxation modulus. For example, at high temperatures, the smaller relaxation modulus would cause the asphalt to deflect more towards the subgrade because of the tire load, whereas its thermal expansion would have an opposite effect. At lower temperatures, the larger relaxation modulus means more resistance to the deformation and thus less deflection in response to mechanical loads; its thermal contraction means a higher deflection. Therefore, according to the deflection curve in *Figure 5-a*, at higher temperatures, it is the relaxation modulus, and at lower temperatures, it is the contraction of asphalt that plays the leading role in the deflection of asphalt.

The tensile strain of asphalt in *Figure 5-b* had a similar trend as its deflection in *Figure 5-a*. It is worthwhile to state that the tensile strain ϵ_x is obtained from the change in horizontal displacements. A large deflection in the y-direction requires the stretch of the material in the x-direction, which corresponds to a larger tensile strain.

In *Figure 6-a*, the deflection of subgrade increased when the temperature of asphalt decreased, and vice versa. The reader is reminded that in the present study, the mechanical properties of subbase layers are not temperature-dependent. So the variation of deflection at point B with temperature change could be due to the changes in the relaxation modulus of the asphalt layer. At low temperatures, the relaxation modulus of asphalt increases and becomes more rigid. This means that the asphalt layer did not dissipate the concentrated deformations under the tire and transmitted the traction force to the underlying layers resulting in a higher deflection.

In general, the ON pavement deflected about 1 mm more than the BC pavement. The reason could be the higher thickness of the pavement in ON compared to the BC pavement model. Therefore, the pavement structure is supported by a thicker elastic material, which resulted in a larger deflection. However, the strains and stresses are very close in both ON and BC because the difference in material properties is minimal, and the applied load is identical.

According to equation (4), the allowable number of load repetitions for fatigue cracking (N_f) depends inversely on the tensile strain (ϵ_t) and the relaxation modulus of the asphalt (E). As temperature rises from about 15 to 40 °C, the tensile strain increases (*Figure 5-b*), while the relaxation modulus decreased (*Figure 5-d*). Therefore, the overall value of N_f depends on which term dominates the equation (4). For temperatures within the 15 to 30 °C, the increase of tensile strain dominates equation (4) and reduces the N_f . After 30 °C, N_f becomes roughly constant (*Figure 8-a*), indicating that the relaxation modulus starts to have a prominent effect. The N_f was significantly reduced when temperature change was outside the designed temperature, i.e. 21 °C (*Figure 8-a*). The N_f was reduced more when temperature decreased compared to when temperature increased. The N_f criterion is not sensitive to temperature change for temperatures over 40 °C, which might be a limitation of this criterion. This indicates that further

investigations are required to validate the fatigue crack criterion for climate conditions with extremely high temperatures.

Figure 8-b shows a mild inverse relation between the N_d and temperature. This is because of the compressive strain ε_y and temperature change are proportionally related, which leads to an inverse relationship between the N_d and temperature in equation (5). It appeared that the permanent deformation criterion is less sensitive to temperature change compared to the fatigue cracking criterion. A comparison of *Figure 8-a* and *8-b* showed that the overall performance of the ON pavement model is slightly better than the BC pavement model. This pavement design is justifiable since ON has a colder season compare to BC.

5. Conclusion

Both failure criteria are of importance in determining the design life of the pavement. However, the effect of climate change, which was presented by temperature change in this study, on the allowable number of load repetitions was more prominent when the fatigue cracking criterion was used. At higher temperatures the permanent deformation predicted a much smaller number of load repetitions than fatigue cracking, while at low temperatures this was the opposite. Therefore, both of these criteria should be taken into account when designing a pavement.

6. Acknowledgment

This project was supported by the National Research Council Canada (NRC) through Climate-Resilient Buildings and Core Public Infrastructure Initiative (CRBCPI) program.

7. Reference

1. Bush E, Lemmen DS: **Canada's changing climate report**: Government of Canada= Gouvernement du Canada; 2019.
2. Van Vuuren DP, Edmonds J, Kainuma M, Riahi K, Thomson A, Hibbard K, Hurtt GC, Kram T, Krey V, Lamarque J-F: **The representative concentration pathways: an overview**. *Climatic change* 2011, **109**(1-2):5.
3. Jahromi SG, Khodaii A: **Effects of nanoclay on rheological properties of bitumen binder**. *Construction and building materials* 2009, **23**(8):2894-2904.
4. Yao H, You Z, Li L, Goh SW, Lee CH, Yap YK, Shi X: **Rheological properties and chemical analysis of nanoclay and carbon microfiber modified asphalt with Fourier transform infrared spectroscopy**. *Construction and Building Materials* 2013, **38**:327-337.
5. Yue Y, Abdelsalam M, Luo D, Khater A, Musanyufu J, Chen T: **Evaluation of the Properties of Asphalt Mixes Modified with Diatomite and Lignin Fiber: A Review**. *Materials* 2019, **12**(3):400.
6. ARA I, ERES Consultants Division.: **Guide for Mechanistic–Empirical Design of New and Rehabilitated Pavement Structures**. *Final Rep, NCHRP Project 1-37A* 2004.

7. <https://infopave.fhwa.dot.gov/Data/DataSelection>
8. Gutierrez-Lemini D: **Engineering viscoelasticity**: Springer; 2014.
9. Tarefder RA, Rahman A: **Interconversion of dynamic modulus to creep compliance and relaxation modulus: numerical modeling and laboratory validation-final report**. In.: University of Nevada, Reno. Solaris University Transportation Center; 2016.
10. MERO M: **Ontario's Default Parameters for AASHTOWare Pavement ME Design Interim Report**. 2019.
11. Logan DL: **A first course in the finite element method**: Cengage Learning; 2011.
12. Huang YH: **Pavement analysis and design**. 2004.